

Precipitative Growth Templated by a Fluid Jet

David A. Stone,[†] Braddon Lewellyn,[‡] James C. Baygents,^{§,⊥} and
Raymond E. Goldstein^{*,‡,⊥,#}

*Department of Soil, Water, and Environmental Science, Department of Physics, Department of
Chemical and Environmental Engineering, Program in Applied Mathematics, and BIO5
Institute, University of Arizona, Tucson, Arizona 85721*

Received July 28, 2005. In Final Form: October 7, 2005

Tubular growth by chemical precipitation at the interface between two fluids, a jet and its surroundings, underlies the development of such important structures as chimneys at hydrothermal vents. This growth is associated with strong thermal and/or solute gradients localized at those interfaces, and these gradients, in turn, often produce radial compositional stratification of the resulting tube wall. A fundamental question underlying these processes is how the interplay between diffusion, advection, and precipitation determines the elongation rate of the tubes. Here we report experimental and theoretical results that reveal a regime in which there exists a new scaling law for tube growth. The model system studied consists of a jet of aqueous ammonia injected into a ferrous sulfate solution, precipitating iron hydroxides with varying oxidation states at the jet boundary. Despite the complex chemistry and dynamics underlying the precipitation, the tube growth exhibits a strikingly simple scaling form, with characteristic lengths and times increasing linearly with the mean velocity of the jet. These observations follow from a kinetic model of advection-dominated flows.

Natural and artificial¹ mechanisms by which tubular structures form often rely upon preexisting, static templates that direct precipitation or mineralization. Less commonly known are growth processes occurring on *dynamic* templates, which define an area of emerging importance within the fields of fluid dynamics and pattern formation: free-boundary problems in precipitative growth. Examples include chemical gardens^{2–4} grown in silicate solutions, tubular growth templated by bubbles^{5,6} or evaporation-driven growth,⁷ and speleothem growth dynamics in limestone caves^{8,9} with connections to the growth dynamics of icicles.^{10,11} Here we address the question, How does a tubular structure grow when precipitation occurs at the boundary between an injected jet of fluid and its surrounding fluid? At hydrothermal vents,¹² the injected fluid and its surroundings differ by two diffusible quantities: thermal energy and solute concentration.^{13,14} The

injected fluid flow is often highly turbulent,¹⁵ but slow, laminar flows are also known. In light of the difficulty in studying such processes in situ, we propose here that a quantitative understanding of this class of phenomena will best be achieved through the development of highly controlled model systems. A few such examples have been introduced,¹⁶ but they have not been explored systematically. An important exception is the study of so-called “ice stalactites”,^{17,18} which form around descending saline plumes under sea ice. Laboratory investigations have shown that a simple diffusive growth law emerges from the combination of double diffusion (heat and salinity) and solidification.

Our system (Figure 1a) consists of a jet of aqueous ammonia that is injected via a syringe pump (New Era Pump Systems N1000) through a 21-gauge needle (radius $a = 0.025$ cm) affixed at the base of a glass chamber ($5 \times 5 \times 30$ cm) in which resides a 0.08 M FeSO₄ solution adjusted with H₂SO₄ to pH 2.3. The volumetric flux Q of ammonia solution in our experiments is typically in the range of several milliliters/hour. Once the fluid exits the nozzle, its velocity profile is nearly constant over its cross section, which is in contrast to ordinary pipe flow with rigid sidewalls. This follows from the fact that the porous tube walls cannot support appreciable shear stress. It is useful to speak of the average fluid velocity, $u = Q/\pi a^2$, which here corresponds to velocities in the range of several millimeters/second. On the scale of the jet radius, the Reynolds number, $Re = ua/\nu$ (in which $\nu = 0.01$ cm²/s is the kinematic viscosity of water), is variable from somewhat less than unity to somewhat greater but is well within the laminar range for the studies reported here. Images

* Corresponding author. Phone: (520) 621-1065; fax: (520) 621-4721; e-mail: gold@physics.arizona.edu.

[†] Department of Soil, Water, and Environmental Science.

[‡] Department of Physics.

[§] Department of Chemical and Environmental Engineering.

[⊥] Program in Applied Mathematics.

[#] BIO5 Institute.

(1) Davis, S. A.; Burkett, S. L.; Mendelson, N. H.; Mann, S. *Nature* **1997**, *385*, 420–423.

(2) Cartwright, J. H. E.; Garcia-Ruiz, J. M.; Novella, M. L.; Otalora, F. *J. Colloid Interface Sci.* **2002**, *256*, 351–359.

(3) Thouvenel-Romans, S.; Steinbock, O. *J. Am. Chem. Soc.* **2003**, *125*, 4338–4341.

(4) Thouvenel-Romans, S.; van Saarloos, W.; Steinbock, O. *Europhys. Lett.* **2004**, *67*, 42–48.

(5) Stone, D. A.; Goldstein, R. E. *Proc. Natl. Acad. Sci. U.S.A.* **2004**, *101*, 11537–11542.

(6) Thouvenel-Romans, S.; Pagano, J. J.; Steinbock, O. *Phys. Chem. Chem. Phys.* **2005**, *7*, 2610–2615.

(7) Stone, H. A.; Du, R. *Phys. Rev. E* **1996**, *53*, 1994–1997.

(8) Short, M. B.; Baygents, J. C.; Beck, J. W.; Stone, D. A.; Toomey, R. S.; Goldstein, R. E. *Phys. Rev. Lett.* **2004**, *98*, 018501.

(9) Short, M. B.; Baygents, J. C.; Goldstein, R. E. *Phys. Fluids* **2005**, *17*, 083101.

(10) Ogawa, N.; Furukawa, Y. *Phys. Rev. E* **2002**, *66*, 041202.

(11) Ueno, K. *Phys. Rev. E* **2004**, *69*, 051604.

(12) Corliss, J. B.; Dymond, J.; Gordon, L. I.; Edmond, J. M.; von Herzen, R. P.; Ballard, R. D.; Green, K.; Williams, D.; Bainbridge, A.; Crane, K.; van Andel, T. H. *Science* **1979**, *203*, 1073–1083.

(13) Tivey, M. K.; McDuff, R. E. *J. Geophys. Res.* **1990**, *95*, 12617–12637.

(14) Tivey, M. K. *Geochim. Cosmochim. Acta* **1995**, *59*, 1933–1949.

(15) Rona, P. A.; Bemis, K. G.; Silver, D.; Jones, C. D. *Mar. Geophys. Res.* **2002**, *23*, 147–168.

(16) Turner, J. S.; Campbell, I. H. *Earth Planet. Sci. Lett.* **1987**, *82*, 36–48.

(17) Martin, S. *J. Fluid Mech.* **1974**, *63*, 51–79.

(18) Perovich, D. K.; Richter-Menge, J. A.; Morison, J. H. *J. Glaciol.* **1995**, *41*, 305–312.

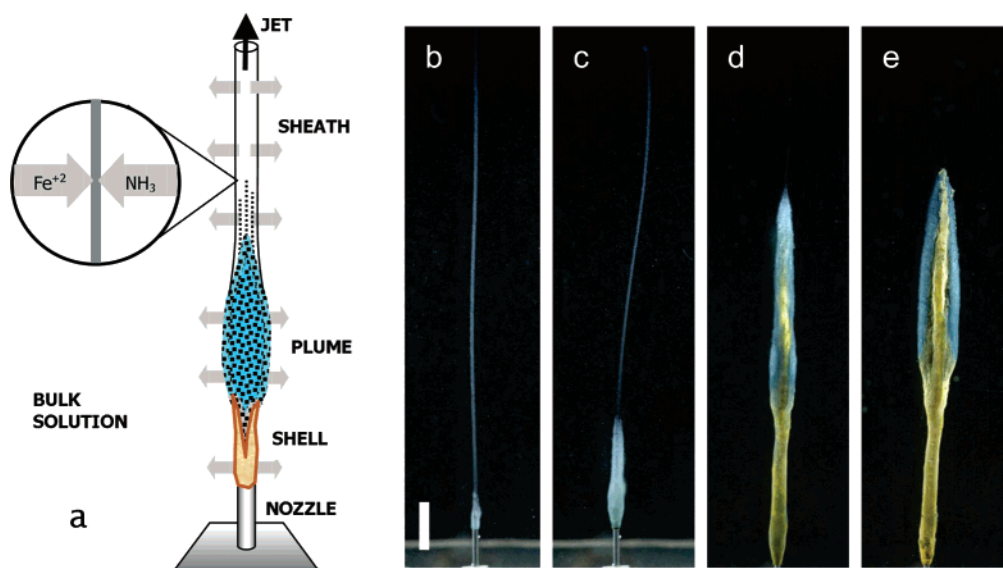


Figure 1. Precipitation templated by a fluid jet. (a) Schematic representation of the stages of growth around a jet of aqueous ammonia injected into an iron sulfate solution, and the subsequent oxidation of the precipitate. (b) 1 min after start, (c) 5 min, (d) 45 min, and (e) 125 min. Scale bar is 5 mm.

of growing tubes were captured with a 12 bit ccd camera (Hamamatsu C848405-G, 1280 × 1024 pixels) and a digital SLR (Nikon D100) with macro lenses, under fiber-optic illumination, and with Schlieren imaging.¹⁹

The growth of the tube results from a complex combination of diffusion, convection, precipitation, and oxidation. It begins when the outward diffusion of OH⁻ and NH₃ from the columnar jet raises the pH in the surrounding acidic ferrous sulfate solution. No tubes form if the pH of the jet is below ~10.5, which is surprising, because dissolved Fe(II) typically precipitates at a pH of ~6. Equally noteworthy is the fact that we do not see tubular growth using NaOH at similar and even higher pH. These observations suggest that the NH₃/NH₄⁺ ratio is critical. It is a function of pH and rises logarithmically above 1 in our system at ~pH 9.3. At a similar value, blue ferrous hexaammine complexes are known to form,²⁰ implying that a minimum concentration of NH₃ as a ligand for complexation is also necessary for tube formation.

As shown in Figure 1, the jet and its enveloping precipitate display three distinct regions. As the jet first rises through the chamber, it is immediately encased by a diaphanous porous white film that can confidently be identified as ferrous hydroxide or “white rust” [Fe(II)-(OH)₂].^{21,22} Much of the film is advected away by the flowing jet, but a flame-shaped plume composed of a cohesive flocculant grows slowly (over tens of minutes) beneath it, which is typically white at first but then gradually turns bluish. The jet flows nearly unimpeded upward through this highly porous precipitate, and even viscously entrains fluid outside the tube, so that its streamlines closely follow the outline of the tube,²³ producing a shear flow.²⁴ This shear is sufficiently strong that the advancing front of dendritic precipitate may occasionally break off from the jet, only to form again later (Figure 2). Further behind,

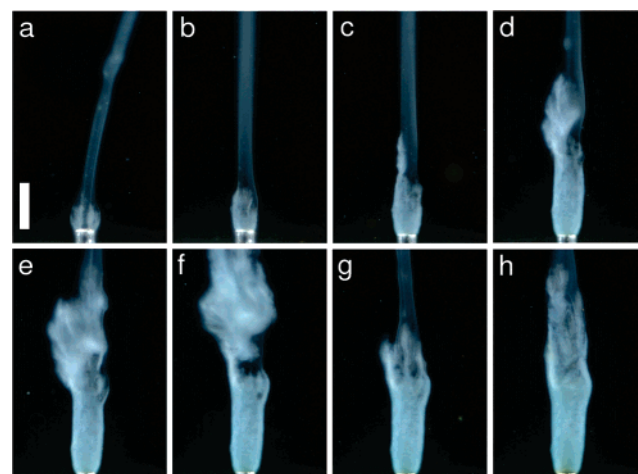


Figure 2. Close-up of a growing tube. The sequence of images spans 5 min, with panels d–g taken 15 s apart. Tube growth begins in (a) as crystallites attach to nozzle, followed by transient elongation (b–d), detachment of a section (e,f), and finally, regrowth (g,h). Scale bar is 2 mm.

the flocculant oxidizes in a sequence that is common at other sites where redox gradients are found. First, ‘green rust’ [Fe(II)₄Fe(III)₂(OH)₁₂SO₄ · nH₂O] quickly appears, then orange lepidocrocite [γ-Fe(III)OOH] slowly takes over. Black blotches and streaks indicate magnetite [Fe(II)Fe(III)₂O₄], a species of intermediate oxidation. The oxidation causes the tube wall to become denser and more rigid, contributing to its structural stability. Over time, the precipitated wall thickens as ammonia diffuses outward and the acidic bulk solution diffuses inward. Eventually, lateral growth ceases. The common feature between this process and the growth of silicate gardens is transport through the tube wall. In the latter case, however, an *inward* flux of water and hydroxide ions is driven by an osmotic stress across the semipermeable wall.

Growth of the tube slows down dramatically at late times, eventually ceasing at a maximum height and after an induction time, which both increase with the jet velocity (Figure 3a). We found that the data can be collapsed to a common curve (Figure 3b) by seeking a maximum height h^* and a time τ (chosen here as the time when $h = 0.6 h^*$)

(19) Pesci, A. I.; Porter, M. A.; Goldstein, R. E. *Phys. Rev. E* **2003**, 68, 056305.

(20) Osseo-Asare, K. *Trans. Inst. Min. Metall., Sect. C* **1981**, 90, C159–C163.

(21) Génin, J. M. R.; Olowe, A. A.; Refait, P.; Simon, L. *Corros. Sci.* **1996**, 38, 1751–1762.

(22) Refait, P.; Bon C.; Simon, L.; Bourrié, G.; Trolard, F.; Bessière, J.; Génin, J. M. R. *Clay Miner.* **1999**, 34, 499–510.

(23) Adler, P. M. *J. Colloid Interface Sci.* **1981**, 81, 531–535.

(24) Adler, P. M. *J. Colloid Interface Sci.* **1981**, 83, 106–115.

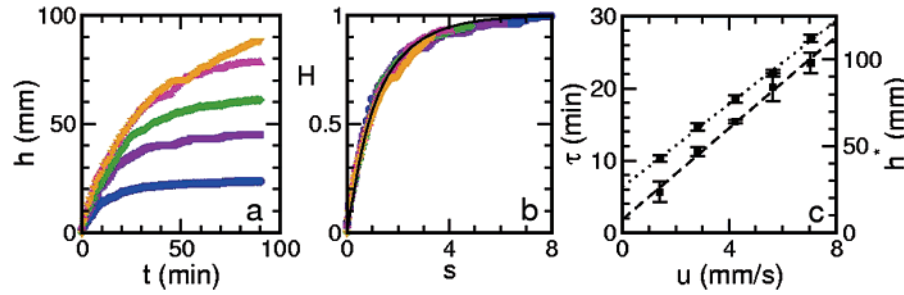


Figure 3. Growth dynamics of tubes. (a) Height vs time at various flow rates: 1 mL/hr (blue) to 5 mL/hr (orange). Each of the growth curves represents the average of three individual runs. (b) Rescaled height H as a function of rescaled time s . Function shown in black is from model described in text. (c) Characteristic time (circles) and maximum height (squares) as functions of average fluid velocity of the jet. Linear fits also shown.

to rescale the data as $H = h/h^*$ versus $s = t/\tau$. Both h^* and τ exhibit simple linear variations with the jet velocity u (Figure 3c). The fundamental mechanism behind the asymptotic saturation of the tube height is the gradual diffusive reduction in the pH of the jet as it rises, coupled with the existence of a critical pH below which precipitation ceases. Ammonia diffuses outward from the flowing jet into the surrounding fluid (Figure 1) through the advancing porous tube wall. The outer ferrous sulfate solution acts as an infinite acidic reservoir, providing a constant source of reactants for the neutralization of the influent stream of ammonia and precipitation. If we follow a parcel of fluid in the rising jet, we will see its pH progressively decrease through this lateral diffusion. A simple model of these processes focuses solely on the hydroxyl concentration C in the ascending fluid jet, taking the rate of precipitative addition to the tube length as being proportional to the concentration C in excess of the critical value C^* . If we assume that C is the same order of magnitude as C^* , then the concentration of hydroxyl ions in the fluid parcel will diminish to C^* on the diffusive time scale a^2/D . Because precipitation ceases once C falls below C^* , h^* should be $\sim ua^2/D$, which is the distance the fluid parcel rises during the interval a^2/D . This proportionality between h^* and u is seen in the data (Figure 3c).

The time scale τ , during which h approaches h^* , depends on lateral diffusion processes and on the precipitation and attachment kinetics. Subsuming all details of the latter into a rate constant k , we write

$$\frac{dh}{dt} = k[C(h) - C^*] \quad (1)$$

This simple supersaturation dynamics is common to precipitation kinetics in geophysics and chemistry.²⁵ We take the centerline value of the concentration within the jet as the measure of the reacting concentration relevant to precipitation. The jets and tubes have large aspect ratios, so the fluid flow is nearly parallel. This also reflects the very large Peclet number $Pe = ua/D \approx 10^3$, in which $D = 10^{-5} \text{ cm}^2/\text{s}$ is typical of a solute diffusion constant. We thus approximate the diffusion as having cylindrical symmetry. In elapsed time t , the centerline concentration corresponding to an initial condition in which C had the uniform value C_0 within a disk of radius a is

$$C = C_0[1 - \exp(-a^2/4Dt)] \quad (2)$$

In writing eq 2, we neglect the loss of hydroxyls due to

precipitation and assume that the porous walls offer negligible resistance to lateral diffusion. As the jet rises from the nozzle at a steady, uniform velocity u , the time t during which the outward diffusion has occurred is simply $t = h/u$. Thus,

$$\frac{dh}{dt} = kC^*[\alpha\{1 - \exp(-a^2u/4Dh)\} - 1] \quad (3)$$

where $\alpha = C_0/C^* > 1$ describes the initial excess concentration in the nozzle. Setting $dh/dt = 0$, we find the asymptotic height

$$h^* = \frac{a^2u}{4D \ln\left(\frac{\alpha}{\alpha-1}\right)} \quad (4)$$

As in the experiments (and previous scaling arguments), h^* is linear in the injected fluid velocity. Defining the rescaled length $H = h/h^*$ as in Figure 3b, the characteristic time

$$\tau = \frac{a^2u}{4DkC^* \ln\left(\frac{\alpha}{\alpha-1}\right)} \quad (5)$$

and the dimensionless time $s = t/\tau$, the rescaled equation of motion for the height $H(s)$ can be written in the remarkably compact form

$$\frac{dH}{ds} = \alpha\left[1 - \left(\frac{\alpha-1}{\alpha}\right)^{1/H}\right] - 1 \quad (6)$$

Having been rescaled by a single characteristic time and the maximum height, this growth equation depends on no other dynamical variables and indeed depends only on the constant α fixed by the initial fluid concentrations. In this sense, this scaled equation of motion is formally consistent with the experimentally observed data collapse. In detail, one verifies for $H \ll 1$ the growth $H \approx (\alpha - 1)s$, or $h \approx k(C_0 - C^*)t + \dots$, the linear elongation expected from the initial jet concentration. Conversely, the approach to the asymptotic height is exponential. The only parameter remaining to distinguish one experiment from another is α . Direct numerical integration was used to obtain the fit shown in Figure 3b, with $\alpha = 1.7$. A fit to the data in Figure 3c for the maximum height as a function of mean fluid velocity yields a slope of 13.2 s. Using the jet radius and the fitted value of α we deduce the effective diffusion constant $D = 1.3 \times 10^{-5} \text{ cm}^2/\text{s}$, which is quite consistent with the typical value for a small molecule in aqueous solution and provides a confirmation that the porous walls offer little resistance to diffusion. From the ratio of the

(25) Keller, J. B.; Rubinow, S. I. *J. Chem. Phys.* **1991**, *74*, 5000–5007.

two fitted slopes in Figure 3c we obtain the intrinsic growth rate $kC^* = 4.6$ mm/s. One discrepancy between the model and the data is the existence of a finite intercept of the relaxation time as the jet velocity vanishes. This is the limit in which the assumptions of the model break down, as the Peclet number is no longer large. A more elaborate theory is required in that regime, particularly in light of the complex attachment kinetics shown in Figure 2.

The good agreement between these experiments and the theory suggests a number of avenues for further experimental and theoretical investigation. The diffusive broadening of the tube wall to equilibrium over time and a microscopic explanation for the observed kinetic parameters are both important open problems that require

consideration of the detailed concentration profiles near and within the tube walls. The mechanism discussed here by which a precipitate forms a self-organized porous boundary between flowing fluids may find applications in a variety of contexts, possibly even at the microfluidic scales.²⁶

Acknowledgment. We thank J.S. Wettlaufer for important discussions. This work was supported in part by the NSF ITR program grant PHY0219411.

LA052064Z

(26) Brody, J. P.; Yaeger, P.; Goldstein, R. E.; Austin, R. H. *Biophys. J.* **1996**, 71, 3430–3441.